Brain Research Bulletin 244 (2026) 112064

Contents lists available at ScienceDirect

Brain Research Bulletin

journal homepage: www.elsevier.com/locate/brainresbull

Research report

Prefrontal responses to negative emotional movements in healthy and symptomatic individuals

Ratna Aditya Apsari [a,1], Somi Lee [b,1], Ela li Maizel [b], Hamin Park [b], Hyuntae Jeong [b], Nakyung Lee [b], Young-Gyun Park [a,b,c,d,*]

[a] Program of Brain and Cognitive Engineering, Korea Advanced Institute of Science and Technology (KAIST), 291 Daehak-ro, Yuseong District, Daejeon (34141), Republic of Korea
[b] Department of Bio and Brain Engineering, Korea Advanced Institute of Science and Technology (KAIST), 291 Daehak-ro, Yuseong District, Daejeon 34141, Republic of Korea
[c] Department of Biological Sciences, Korea Advanced Institute of Science and Technology (KAIST), 291 Daehak-ro, Yuseong District, Daejeon 34141, Republic of Korea
[d] KAIST Institute for Health Science and Technology (KIHST), 291 Daehak-ro, Yuseong District, Daejeon (34141), Republic of Korea

ARTICLE INFO

Keywords:
Functional Near Infrared Spectroscopy (fNIRS)
Emotional movements
Depression
Prefrontal cortex

ABSTRACT

Brain-body interaction is central to emotion. For example, emotional bodily movements not only express emotions but also evoke associated emotional states. However, a mechanistic understanding of how emotional movements influence our mood remains elusive due to the challenge of recording brain activity in moving subjects. Here, we used wireless functional Near Infrared Spectroscopy (fNIRS) to investigate how emotional movements modulate prefrontal activity in healthy (low PHQ-9) and symptomatic (high PHQ-9) subjects. We found that imitating negative emotional movements commonly activates the left anterior prefrontal cortex in healthy subjects. In contrast, the same movements deactivate this region in subjects with elevated depressive symptoms, revealing an opposite prefrontal response between groups. In an exploratory follow-up, PHQ-9 scores assessed 1–2 weeks later increased in healthy subjects and decreased in symptomatic subjects; however, this change tracked baseline symptom severity irrespective of movement valence and thus can be a result of regression to the mean, and is therefore reported with caution. This research suggests that the left anterior prefrontal cortex is associated with brain–body interaction during negative emotional movements, and that this prefrontal response differs markedly in individuals with elevated depressive symptoms.

1. Introduction

Humans express emotions through emotional behaviors such as facial expressions (e.g., frowning, smiling) and bodily movements (e.g., skipping, drooping shoulders). However, emotional behaviors can also induce emotional states (Mennin et al., 2007). For example, imitating positive emotional behaviors induces positive emotions, whereas imitating negative emotional behaviors provokes negative emotions (Duclos and Laird, 2001; McIntosh, 1996; Shafir, 2016; Shafir et al., 2013). Moreover, imitating emotional behaviors is used as a way to regulate mood in therapeutic settings (Laird and Lacasse, 2014; McIntosh, 1996; Shafir et al., 2016). These indicate that a neural mechanism that evokes mood changes upon emotional behaviors might be present.

Several studies reported brain activity changes induced by facial expressions. A neuroimaging study reported characteristic brain activity changes during the imitation of facial expressions for anger, sadness, or happiness (Lee et al., 2006). Moreover, Hennenlotter et al. (2009) found that injecting botulinum toxin into frown muscles, which are commonly contracted during negative facial expressions (Finzi and Rosenthal, 2016), reduced activity in the left amygdala, a brain area associated with negative emotion processing. As an origin of these brain activity changes by facial expressions, proprioceptive feedback of facial expression has been suggested (Finzi and Rosenthal, 2016).

Emotional bodily movements evoke specific patterns of proprioceptive feedback signals (Damasio and Carvalho, 2013; Ackerley et al., 2017). For example, negative emotional movements such as drooping

* Corresponding author at: Program of Brain and Cognitive Engineering, Korea Advanced Institute of Science and Technology (KAIST), 291 Daehak-ro, Yuseong District, Daejeon 34141, Republic of Korea.
E-mail address: ygpark12@kaist.ac.kr (Y.-G. Park).
[1] These authors contributed equally to this work.

https://doi.org/10.1016/j.brainresbull.2026.112064
Received 11 February 2026; Received in revised form 16 July 2026; Accepted 30 July 2026
Available online 31 July 2026

shoulders or hugging knees are characterized by shrinking postures and slumped torso (Shafir, 2015), which generate a characteristic pattern of proprioceptive feedback signals (Damasio and Carvalho, 2013; Ackerley et al., 2017). The proprioceptive feedback signals are conducted to diverse brain regions, for example, to the thalamus and primary somatosensory cortex via the dorsal column-medial lemniscus pathway, or to the cerebellum via spinocerebellar tract. Based on connectivity between brain regions, these proprioceptive signals are supposed to reach the prefrontal cortex and insula, which are important for emotion processing (Diener et al., 2012; Belleau et al., 2019; Khalsa et al., 2018; Aman et al., 2015; Lial et al., 2017). However, in contrast to facial expressions, the neural correlates that translate emotional bodily movements into mood changes have been elusive due to the challenges of recording brain activity from moving human subjects.

Functional Near Infrared Spectroscopy (fNIRS) can record brain activity by measuring local oxygenated hemoglobin concentration using near-infrared light (Ferrari and Quaresima, 2012; Scholkmann et al., 2014). fNIRS is more resistant to motion artifacts than other neuroimaging methods (e.g., EEG, fMRI) since its optrodes are firmly attached to the head (Al-Omairi et al., 2023). Additionally, various hardware- and software-based solutions are developed to remove motion artifacts of fNIRS recording (Huang et al., 2022). Together with the development of wireless and portable fNIRS systems (Pinti et al., 2018, 2020), these properties of fNIRS enabled brain activity monitoring during diverse bodily movements (Pinti et al., 2020).

In this study, we assessed brain activity during emotional bodily movements by using a wireless fNIRS device and a robust fNIRS signal preprocessing, analysis, and validation pipeline. We focused our brain activity recording on the prefrontal cortex (PFC) because of its involvement in emotional processing (Diener et al., 2012) and mood disorders (Belleau et al., 2019; Delaveau et al., 2011). We found that imitating negative emotional movements commonly activates the left anterior prefrontal cortex in healthy subjects. In an exploratory follow-up, depressive symptoms changed after the task—increasing in healthy subjects and decreasing in symptomatic subjects—but this change tracked baseline symptom group rather than movement valence and was consistent with regression to the mean (see Discussion). These results indicate that the left anterior prefrontal cortex shows an opposite task-evoked response to negative emotional movements in healthy versus symptomatic individuals, suggesting their changed role in individuals with elevated depressive symptoms.

2. Methods

2.1. Participants

This study was conducted in accordance with the ethical principles outlined in the Declaration of Helsinki and received approval from the Institutional Review Board of Korea Advanced Institute of Science and Technology (KAIST) on December 4th, 2023 (approval number: KH2023–147).

The general study flowchart is presented in Fig. 1**A**. Among the volunteers in this study, we pre-screened subjects based on inclusion and exclusion criteria. The inclusion criteria are age (ranging from 20 to 35 years old) and Patient Health Questionnaire (PHQ−9)(Kroenke et al., 2001) score (ranging from 0 to 2 or ranging from 5 to 19) (Beard et al., 2016). Subjects diagnosed with major psychiatric symptoms during the last two years, having physical impairments interfering with the execution of behavior tasks used in this study, or using psychoactive medication (e.g., antidepressants) were excluded.

Subjects who passed the pre-screening went through the subsequent psychiatric interview. A licensed researcher interviewed prospective subjects to assess the severity of depression and anxiety, alongside screening for other psychiatric conditions using the Modified MINI Screen (MMS)(Sheehan et al., 1998), thereby validating the pre-screening results.

The pre-screening and screening procedure resulted in 52 subjects. Because groups were defined by questionnaire screening (PHQ−9 and the Modified MINI Screen) rather than clinical diagnosis, we refer to the PHQ−9 ranging 5–19 group as the symptomatic group (elevated depressive symptoms) rather than as clinically depressed. The sample comprised 27 healthy subjects (PHQ−9 ranging from 0 to 2) and 25 symptomatic subjects (PHQ−9 ranging from 5 to 19). The subjects consisted of 32 males and 20 females. The ‘male’ and ‘female’ refer to the biological sex assigned at birth based on anatomical and physiological characteristics. This experiment was approved by the written informed consent forms obtained from all subjects prior to starting the experiment. All subjects agreed to have their personal information and brain recordings used for research purposes. While a total of 52 participants (27 healthy and 25 symptomatic) were initially enrolled in the study, the final sample sizes for the analyses reported in the Results section may vary. This fluctuation in subgroup sample sizes was due to technical data acquisition issues (specifically, missing estimates during fNIRS preprocessing for one healthy and two symptomatic subjects) and participant attrition during the follow-up period.

2.2. Experimental design

The experimental tasks were divided into two categories: positive and negative emotional movements. Positive emotions are associated with feelings of joy, pleasure, excitement, inspiration, or happiness, while negative emotions encompass feelings of despair, sadness, contempt, guilt, or nervousness (Shafir, 2015). The positive and negative emotion-expressing movements were chosen based on previous publications (see Table 3; Fig. 1**B**).

The experiments were conducted in an isolated room to reduce external distractions and improve focus. Prior to starting the experiment, subjects were given a short briefing of the experiment, in which researchers explained the device, experimental design, task instructions and showed demonstration videos of the task movements to the subjects. Subjects from each group (healthy or symptomatic) were randomly assigned to either a positive emotional movement group or a negative emotional movement group and asked to do a set of either positive emotional movement tasks or negative emotional movement tasks according to their task group assignment. Task cues were visually shown on a monitor in front of the subjects, showing a screenshot of the particular task movement (Fig. 1**C**). Subjects were instructed to maintain a state of calm and focused relaxation throughout the tasks. Precautions were taken for subjects experiencing sleepiness or fatigue as it may alter cerebral hemodynamics (Oniz et al., 2019).

As illustrated in the experimental design in Fig. 1**D**, each subject completed only one type of emotional movement set (positive or negative) throughout the entire experiment to ensure that there was no cross-contamination or carry-over effects between the positive and negative emotional conditions. Each movement task was repeated four times in sub-sessions or “blocks”. Thus, all participants in each group (positive or negative movement set) completed a total of 12 individual task trials. For each block, tasks were conducted for 30 s and interleaved with a 60-second resting period (inter-task interval, ITI). In the postprocessing, this ITI period was divided into two parts, the pre-task and the post-task. The pre-task is the period preceding the onset of individual trials and is used as a baseline. The post-task period is the period following individual trials, capturing potential residual effects of the tasks. The sequence of the tasks assigned to each subject was randomized.

2.3. Devices

2.3.1. fNIRS

Data acquisition was carried out using a portable and wireless 21-channel continuous-wave fNIRS device (Fig. 3**A**; NIRSIT Lite, OBELAB, South Korea), which is designed to measure hemoglobin changes in the PFC region. NIRSIT Lite utilizes two light sources (780 and 850 nm) and

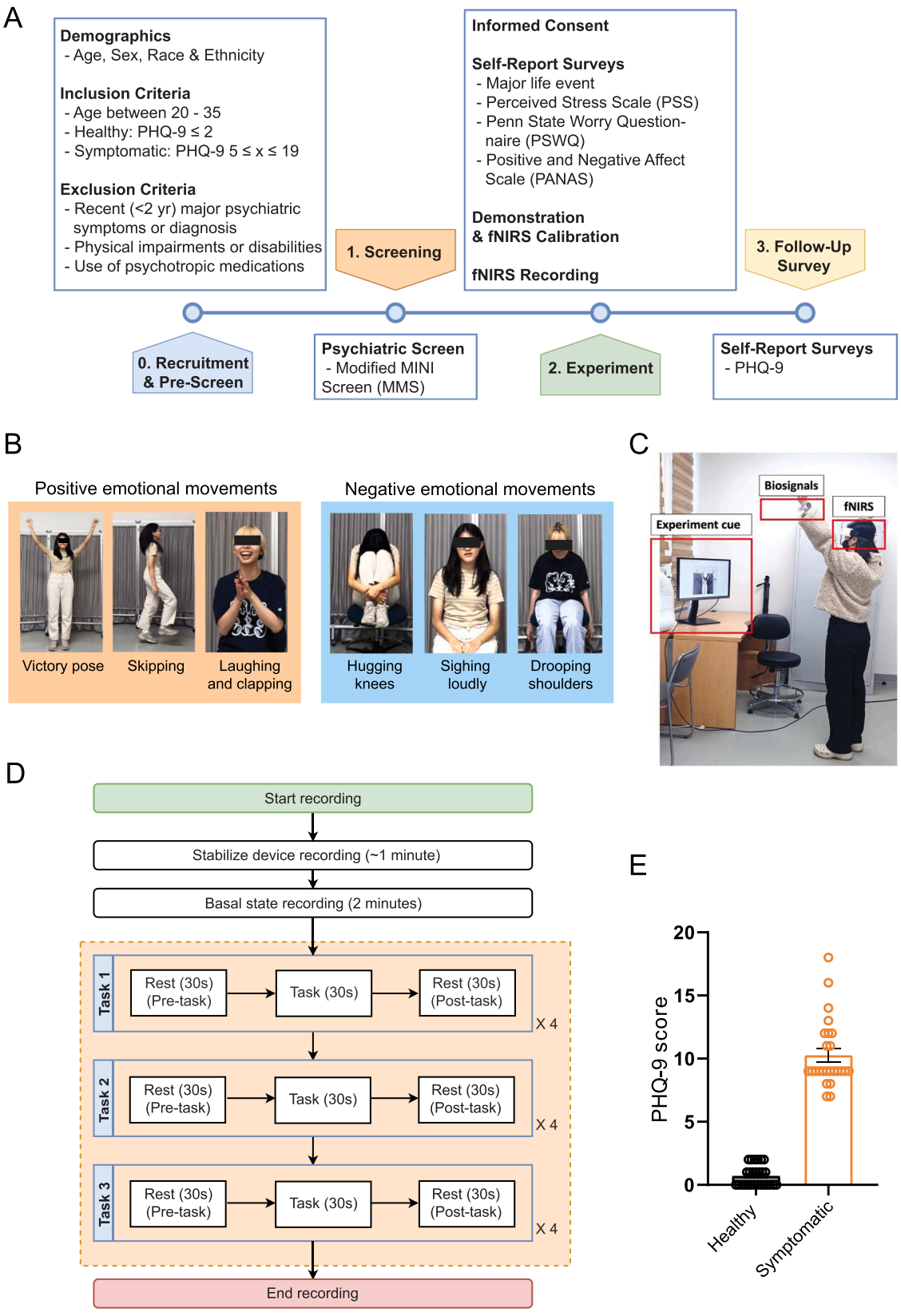

Fig. 1. The experimental design. A) The overall flowchart of this study. B) Emotion-expressing bodily movements used in this study. C) Experimental setup. D) Experimental design of the tasks. E) Baseline PHQ−9 values of the healthy (n = 27) and symptomatic (n = 25) subjects measured before the experiment.

has an 8.138 Hz sampling frequency. This device has three different source-detector distances for channels: long-separation (LS) channels (30 mm distance) and two types of short-separation (SS) channels (7 mm or 15 mm distance). The channel layout of the NIRSIT Lite device is shown in Fig. 3**B**, which indicates the 15 LS channels together with the prefrontal subregions they cover, as specified by the manufacturer for this device. Channel 13, on which our analyses focus, falls within the left anterior prefrontal region of this map. Other than the source-detector channels, the NIRSIT Lite also houses a 6-axis gyroscope and a 3-axis accelerometer, which are useful for analyzing head movements. The estimated MNI coordinates for all 15 LS channels are listed in Table 1. Because these coordinates were derived from the vendor-provided probe geometry rather than from individual anatomical images, and because 15 long-separation channels sample the prefrontal surface only coarsely, channel-level anatomical labels in this study should be regarded as approximate.

2.3.2. Biosignals smartwatch

EmbracePlus (Empatica, USA) is a wearable device for collecting, processing, storing, and wirelessly transmitting physiological parameters. It is designed to be worn on the wrist and equipped with a range of sensors, including an accelerometer, gyroscope, Photoplethysmogram (PPG), and EDA. In this study, data collected by EmbracePlus is transferred to the companion app/system via Bluetooth.

2.4. Preprocessing and analysis

2.4.1. fNIRS

The fNIRS preprocessing and analysis pipeline is shown in Fig. 3**C**. The preprocessing pipeline is constructed to efficiently remove artifacts. Briefly, time-series data of optical intensity were obtained from subjects and converted to NIRS format (Santosa et al., 2018) for ease of processing. Then, signal detrending was applied to remove signal drifts caused by the heating of the device during data acquisition. Afterward, Temporal Derivative Distribution Repair (TDDR) (Fishburn et al., 2019) was applied to remove motion artifacts by implementing robust estimators and effectively correcting shifts in baseline and spike artifacts. Signals were then converted from optical density to Modified Beer-Lambert Law (MBLL) concentrations. A bandpass filter (3rd order Butterworth filter, with a band-pass filtering between 0.01 and 0.2 Hz) was implemented to remove physiological noises derived from respiration, heartbeat, or Mayer waves. Based on the previous publication supporting that oxygenated hemoglobin concentration is a good proxy for brain activity (Obrig et al., 2000; Pinti et al., 2015), we focused on analyzing the oxygenated hemoglobin (HbO) signals in this study using a General Linear Model.

Table 1
Estimated MNI coordinates of the 15 channels of the NIRSIT Lite device. X, Y, and Z values represent coordinates in MNI space, where X denotes the left-right axis (negative = left hemisphere), Y denotes the anterior-posterior axis, and Z denotes the superior-inferior axis. Location indicates the hemispheric position of each channel. MNI, Montreal Neurological Institute. MNI coordinates were provided by OBELAB, Inc. (Seoul, South Korea).

Channel	X	Y	Z	Location
CH 1	54.67	44.00	0.00	Right
CH 2	48.00	52.67	12.67	Right
CH 3	36.33	58.33	24.67	Right
CH 4	39.00	64.67	0.00	Right
CH 5	26.33	69.67	12.67	Right
CH 6	13.67	69.00	24.67	Right
CH 7	14.33	73.00	0.33	Right
CH 8	0.33	68.00	11.33	Center
CH 9	−13.00	68.00	24.00	Left
CH 10	−14.33	73.00	0.00	Left
CH 11	−26.00	68.00	12.00	Left
CH 12	−35.67	57.67	23.67	Left
CH 13	−38.00	63.00	0.00	Left
CH 14	−45.67	51.67	12.33	Left
CH 15	−52.33	43.67	−0.33	Left

General Linear Model (GLM) is a well-known method in neuroimaging for obtaining brain activation maps from statistical parametric mapping (Tak and Ye, 2014). For the segmentation and analysis of the task data, we utilized NIRS Brain AnalyzIR toolbox (Santosa et al., 2018). Given that fNIRS obtains brain hemodynamic data from the surface of the head, it is susceptible to signal contamination from scalp blood flow, or "global component". To address this issue, Santosa et al. utilized a regression model incorporating data from SS channels as regressors within the GLM network to effectively remove systemic contaminations (Santosa et al., 2020). This regression model combines the mixed effects model, autoregressively iterative robust least squares (AR-IRLS), and short-separation channel regression. SS channel data is essential for eliminating global systemic contamination because the data majorly reflects scalp hemodynamic activities, which are supplied by the external carotid arteries (Wyser et al., 2020, 2022). Incorporating SS channel measurements as an additional regressor within the GLM ensures the effective removal of global systemic contaminations from the LS channels.

To process the SS channels as the regressors in the GLM, we first defined X_{short} as the HbO or HbR signal of the SS channels and X_{task} as the observed HbO or HbR signal in the LS channel. Therefore, we could describe the regression model as follows (Santosa et al., 2020):

$$Y = [X_{task}\ X_{short}] \bullet \begin{bmatrix} \beta_{task} \\ \beta_{short} \end{bmatrix} + \varepsilon$$

where β_{task} represents the strength of task activation and β_{short} represents the strength of SS channel activity, with ε as the error term. For each LS channel, the weights of the SS regression are determined individually.

In the mixed effects regression model, the initial equation is modified to the following equation:

$$Y = \quad X_{task} \bullet \beta + \quad Z_{short} \bullet \Gamma + \quad \varepsilon$$

where Z_{short} is a renamed version of X_{short} to clarify the terminology within the mixed effects framework. Here, β represents the fixed effects coefficient, Γ denotes the random effects coefficient, and ε is the error term. The statistical significance of the results derived from the GLM was calculated using the Benjamini-Hochberg FDR-corrected q-value (Santosa et al., 2018). In this study, the direction and magnitude of the β coefficient of HbO were used as a proxy of direction (positive or negative)(Baker et al., 2018) and the intensity of cerebral activity, respectively (Gu et al., 2017).

2.4.2. Biosignals smartwatch

The data processing pipeline for the Empatica EmbracePlus, as shown in Supplementary Fig. 1, mainly focuses on the EDA data processing. Initially, raw data are collected and stored in Avro files, which are then preprocessed and converted to CSV format for easier handling. To indicate the experiment duration, the 'TAGS' column was added based on the closest Unix timestamps based on the subject's physical tagging during the experiment. For artifact removal, the EDA data was further processed with the Ledalab toolbox (Benedek and Kaernbach, 2010) to manually eliminate motion artifacts through visual inspection (Caruelle et al., 2019). After artifact correction, we applied Continuous Decomposition Analysis to extract continuous phasic and tonic activity, which yielded the Skin Conductance Response (SCR). Detailed processes of the preprocessing and analysis pipeline are described in Supplementary Fig. 1B.

2.4.3. Post-hoc sensitivity analysis

After data collection was completed, we conducted a post-hoc sensitivity analysis in RStudio (package pwr, v2025.09.2 +418) to quantify the minimum detectable effect sizes (MDEs) for two-sample

comparisons at α = .05 (two-sided) and 80% power. Because group classification (healthy vs. symptomatic) was defined by PHQ−9 scores, the PHQ−9 group difference is circular and was not used as a sensitivity benchmark; the sensitivity analysis therefore concerns the hemodynamic (β) comparisons only. For the emotional movement comparisons, each subject from the healthy or symptomatic group performed either negative or positive emotional movement tasks. Therefore, individual β values obtained from the first-level GLM analyses were used as proxy measures of the effect size for hemodynamic activity and were analyzed separately for the negative task group (Healthy, number of subjects = 13; Symptomatic, number of subjects = 13) and positive-task group (Healthy, number of subjects = 13; Symptomatic, number of subjects = 10).

2.5. Questionnaire

Prior to the experiment, subjects were asked to fill out self-report questionnaires. In addition to PHQ−9 and the Generalized Anxiety Disorder−7 (GAD−7; Spitzer et al., 2006), subjects completed the Perceived Stress Scale (PSS) (Cohen et al., 1983), Penn State Worry Questionnaire (PSWQ)(Meyer et al., 1990), and Positive and Negative Affect Schedule (PANAS; Watson et al., 1988). Particularly, PANAS is a self-assessment questionnaire that measures positive and negative affect on a 1–5 Likert scale, consisting of 20 different words (e.g., *interested, distressed*) that could describe a person's subjective feelings and emotions (Magyar-Moe, 2009). PANAS has been widely used in clinical and non-clinical studies because of its validity and reliability in assessing the nuanced state of positive and negative affect (Merz et al., 2013). These self-report measures were administered prior to the movement tasks to confirm the validity of participant group assignment (healthy vs. symptomatic) and to screen for any potential outliers that could influence subsequent analyses.

3. Results

3.1. Experimental design and demographics

The overall experimental flowchart of the study is shown in Fig. 1**A**. Fifty-two subjects (27 healthy and 25 symptomatic subjects) passed prescreening and screening processes and participated in this study. The mean scores of PHQ−9 for healthy and symptomatic subjects were 0.7 and 10.28, respectively (Fig. 1**E**). Detailed descriptive statistics of the baseline mood parameters are described in **Table 2**. Between-group comparisons using Welch's two-sample *t*-test revealed significant differences in PHQ−9, GAD−7, PSS, PANAS(PA), and PANAS(NA) between healthy and symptomatic subjects (all $p < .05$), whereas age, PSWQ, baseline EDA, and baseline SCR did not differ significantly between groups (Table 2).

The emotional bodily movements used in this study were chosen based on the previous publications (Table 3). We chose emotion-expressing movements that are relevant to positive emotions (positive emotional movements) or negative emotions (negative emotional movements) (Fig. 1**B**). Subjects watched videos and read text guides to imitate a set of either positive or negative emotional movements (Fig. 1**C**) and performed the set of the movements 4 times repetitively, for total duration of 6 min (Fig. 1**D**) while their PFC activity and biosignals were recorded by fNIRS and biosignal smartwatch, respectively.

3.2. Correlation analysis of the baseline mood parameters

We analyzed the correlation among the baseline mood parameters in healthy and symptomatic subjects (Fig. 2). We observed statistically significant positive correlations between the subject groups (Healthy = 0, Symptomatic = 1) and PHQ−9, GAD−7, and PSS, suggesting that the symptomatic group has higher depressive mood, anxiety, and stress levels compared to healthy group, which is consistent to previous studies (Odero et al., 2023). The symptomatic group also showed significantly lower PANAS positive affect and higher PANAS negative affect compared to the healthy group. Likewise, higher PHQ−9 was associated with higher anxiety, stress, worry, and PANAS negative affect, as well as with lower PANAS positive affect. The basal stress level was positively correlated with worry and PANAS negative affect, whereas it was negatively correlated with the baseline measure of EDA. Together, these patterns of correlations suggest that symptomatic subjects were consistently associated with elevated scores on standardized measures of depression, anxiety, stress, and negative affect, and also with low scores on positive affect, supporting our classification of healthy and symptomatic subject groups and cross-confirming our baseline measurements.

Table 3
Positive and negative emotional bodily movements used in this study.

Positive emotional movements	Short names	Negative emotional movements	Short names
Fully stretching both arms in the air, such as in the gestures we make when we celebrate a victory (Coulson, 2004; Melzer et al., 2019)	Victory pose	Sitting down on a chair while hugging the knees and dropping the head (Melzer et al., 2019; Shafir, 2015; Veenstra et al., 2016)	Hugging knees
Walking with a slight jump, or skipping (Melzer et al., 2019)	Skipping	Sighing loudly (Shafir, 2015)	Sighing loudly
Laughing loudly while clapping (Shafir, 2015)	Laughing while clapping	Drooping one's shoulders with letting the body go limp on a chair (Coulson, 2004; Melzer et al., 2019)	Drooping shoulders

Table 2
Descriptive statistics of baseline measures used in this study. SD, standard deviation; PHQ−9, Patient Health Questionnaire−9; GAD−7, General Anxiety Disorder−7; PSS, Perceived Stress Scale; PSWQ, Penn State Worry Questionnaire; PANAS (PA), Positive and Negative Affect Scale (Positive Affect); PANAS (NA), Positive and Negative Affect Scale (Negative Affect); EDA, electrodermal activity. Between-group comparisons were conducted using Welch's two-sample *t*-test. t, t-statistic; p, two-tailed p-value.

Variable	Healthy		Symptomatic		Between-Group	
	Average	SD	Average	SD	t	p
Age	23.44	2.83	24.44	3.06	−1.215	0.230
PHQ−9	0.7	0.82	10.28	2.7	−17.013	< .0001
GAD−7	0.33	0.62	6.32	3.02	−9.712	< .0001
PSS	13.3	4.83	19.96	5.44	−4.657	< .0001
PSWQ	48.19	9.6	53.52	9.95	−1.965	.055
PANAS(PA)	17.37	6.16	14.12	4.79	2.133	.038
PANAS(NA)	8.81	2.27	12.16	4.79	−3.175	.003
Baseline EDA	1.76	2.85	0.61	0.94	1.263	.230
Baseline SCR	−0.28	0.57	−0.16	0.41	−0.528	.604

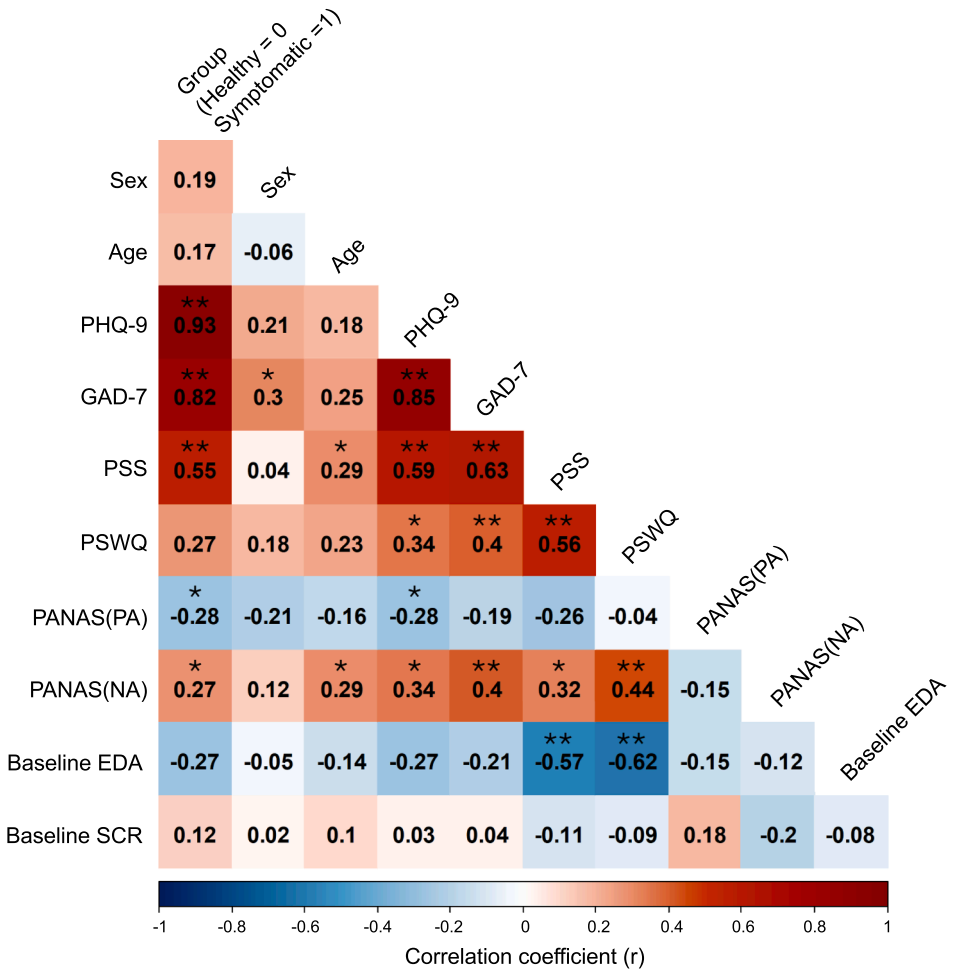

Fig. 2. The correlation matrix of the baseline mood parameters. Numbers indicate correlation coefficients. Two-tailed Pearson correlation test, **P < 0.01, *P < 0.05.

3.3. *Establishment of fNIRS preprocessing and analysis pipeline*

For fNIRS data acquisition, we utilized NIRSIT Lite, a wireless 21-channel fNIRS device (Fig. 3**A**; OBELab, South Korea). The channel map of the device is shown in Fig. 3**B**. For accurate assessment of brain activity using fNIRS, we constructed an fNIRS signal preprocessing and analysis pipeline that includes Temporal Derivative Distribution Repair (TDDR)(Fishburn et al., 2019) for motion artifact removal and a general linear model with short separation channel regressor (GLM-SS)(Santosa et al., 2020) for systemic artifact removal (Fig. 3**C**). The efficient removal of motion artifact by using TDDR was confirmed by comparing fNIRS signals with accelerometer signals recorded simultaneously using the sensor in the fNIRS device (Fig. 3**D**). The quality of brain activity recording by fNIRS was assessed by checking negative correlations between the concentrations of the oxygenized hemoglobin (HbO) and deoxygenized hemoglobin (HbR), which is an established indicator of a successful recording of hemodynamic responses (Lee et al., 2018). We found that HbO and HbR concentrations we measured showed inverse correlation across channels and subjects of this study (Fig. 3**E**).

3.4. *Prefrontal activity changes induced by negative emotional movements*

From the analysis of fNIRS signals, we found that diverse negative emotional movements are associated with a common pattern of prefrontal activity changes (Fig. 4). The maps of the beta coefficient, which reflect the direction and intensity of brain activity changes (Baker et al., 2018; Gu et al., 2017), revealed that all three negative emotional movements (hugging knees, drooping shoulders, sighing loudly) commonly activate the left anterior prefrontal cortex, with the highest degree of activation at its lateral part in healthy subjects (Fig. 4**A**; channel 13). Interestingly, the same movements commonly inactivated the cortical area in symptomatic subjects (Fig. 4**A**). Supporting this, the maps of beta coefficient difference between the healthy and symptomatic subjects showed the highest contrast at channel 13 in all three negative emotional movements (Figs. 4**A** and 4**B**). We also investigated brain activity changes by positive emotional movements; however, a common brain activation pattern was not observed across positive emotional movements (Supplementary Fig. 2). These results suggest that the left anterior prefrontal cortex is involved in negative emotional movement-induced common physiological changes in a contrasting manner between healthy and symptomatic subjects.

3.5. *Delayed changes in depressive symptoms after negative emotional movements*

To investigate the delayed effect of imitating emotional movements on depressive mood, we assessed the depression index (PHQ−9) of the subjects 1–2 weeks after performing the tasks. The PHQ−9 scores of the subjects who performed positive emotional movements on the day of the experiment showed no significant net change in each group (Fig. 5**A**). The subjects who performed negative emotional movements showed a significant PHQ−9 change in each group—healthy subjects increased and symptomatic subjects decreased (Fig. 5**B**). Follow-up PHQ−9 change scores for all four cells were: healthy–negative $\Delta = +1.15$

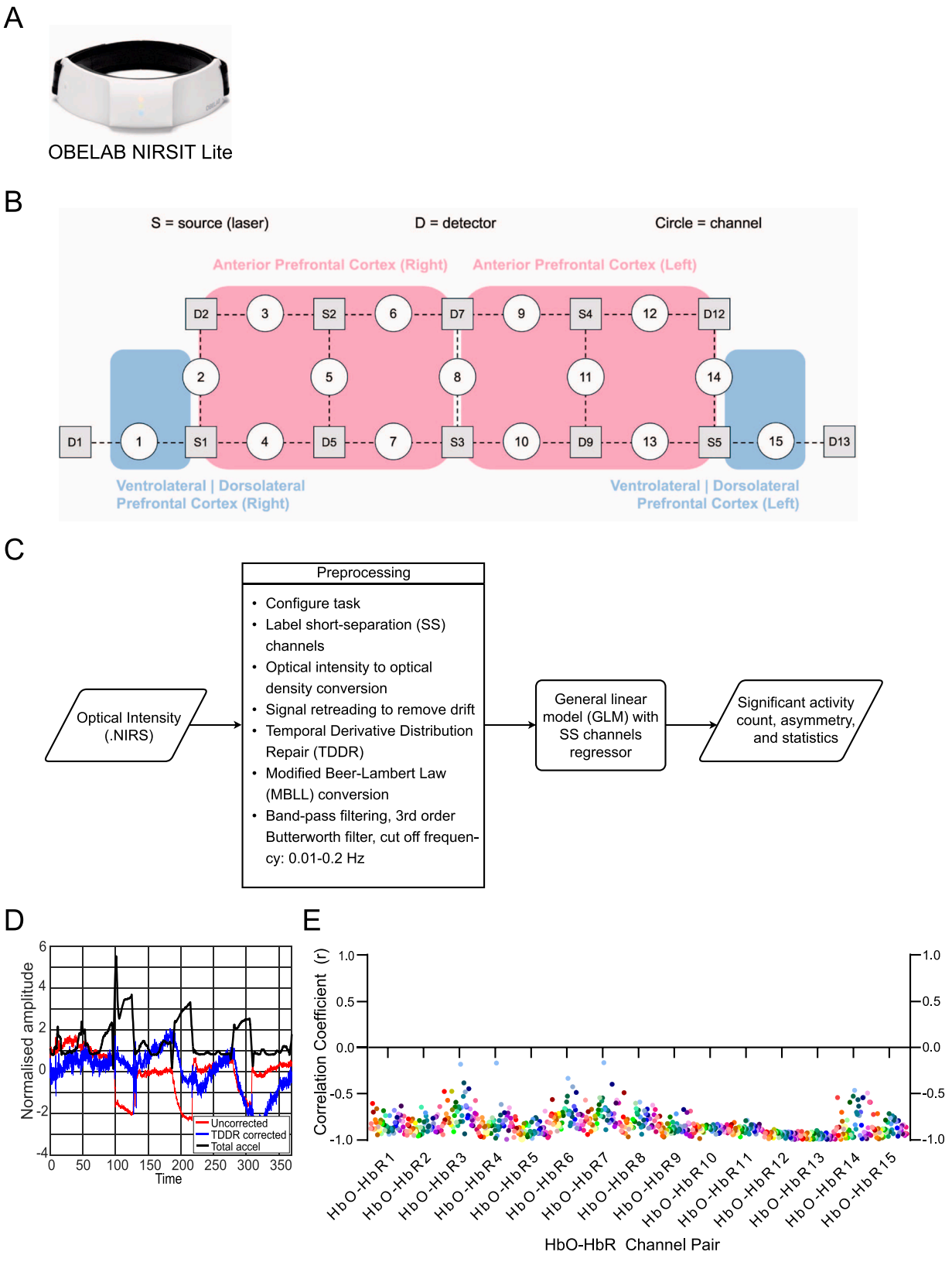

Fig. 3. The hardware, analysis pipeline, and validation of fNIRS recording. A-B) The image (A) and the map (B) of the fNIRS device used in the study. The map of the long-separation channels and light source distribution is presented. S denotes the light source (laser), D denotes the photodetector, and circles indicate measurement channels with a source-detector separation distance of 30 mm. Channel 13 falls within the left anterior prefrontal region. C) The preprocessing and analysis pipeline of fNIRS used in this study. D) Raw optical density signals of fNIRS channel data before (red line) and after (blue line) TDDR motion correction. The black line indicates the total acceleration of the fNIRS device in all three axes, reflecting head movements of the subject. E) Inverse correlation between HbO and HbR signals across fNIRS channels (N = 15) and subjects (N = 52) (Two-way ANOVA, $P < 0.001$). Colors of the dots indicate individual subjects. TDDR, Temporal Derivative Distribution Repair; HbO, Oxygenated hemoglobin; HbR, Deoxygenated hemoglobin.

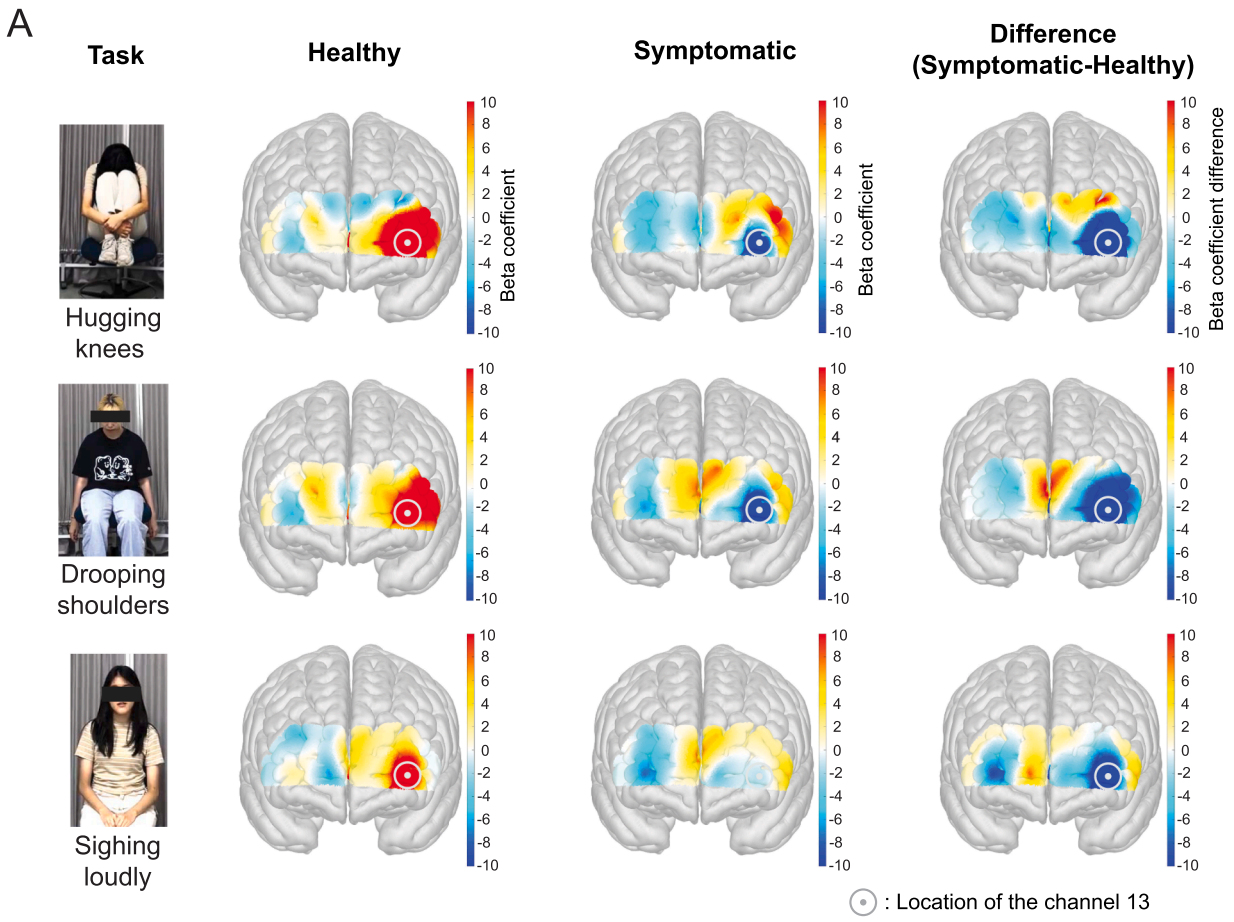

Fig. 4. Brain activity changes during negative emotional movements in healthy and symptomatic subjects. A) 3D beta coefficient maps of healthy (left) and symptomatic subjects (middle) and their differences (right). B) 2D maps of beta coefficient differences of individual negative emotional movements overlaid with the fNIRS channel map. Note that the difference is mostly prominent at channel 13 in all the negative emotional movements. Beta coefficients were estimated with a general linear model including short-separation channel regressors, and statistical significance was assessed using Benjamini–Hochberg FDR-corrected q-values.

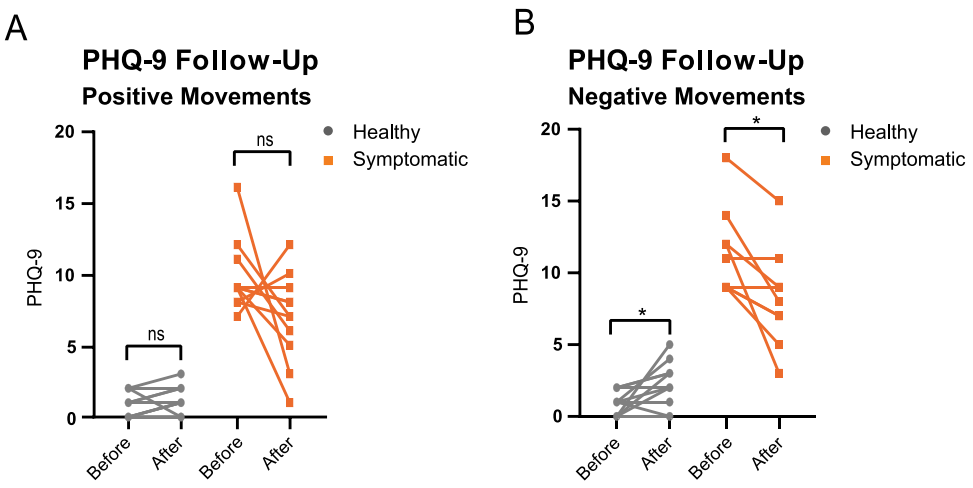

Fig. 5. Changes in PHQ−9 1–2 weeks after positive (A) or negative (B) emotional movements in healthy or symptomatic subjects. Bars indicate mean ± SEM. Within-cell changes were assessed using two-tailed paired *t*-tests: healthy–positive (n = 13), symptomatic–positive (n = 11), healthy–negative (n = 13), and symptomatic–negative (n = 9). ns, not significant; *P < 0.05, **P < 0.01. Change scores and the corresponding test statistics for all four cells are reported in Table 4. Note that the direction of change tracked baseline symptom group in both movement arms; the valence × group interaction was non-significant (3.5).

(n = 13), healthy–positive Δ = + 0.31 (n = 13), symptomatic–negative Δ = −3.22 (n = 9), and symptomatic–positive Δ = −2.82 (n = 11) in average (Table 4). Symptomatic subjects therefore decreased and healthy subjects increased in both movement arms, so the direction of change tracked baseline symptom group rather than movement valence. A 2 (group) × 2 (valence) analysis confirmed a large main effect of group ($F(1, 42) = 18.6$, $p < .001$) but no valence × group interaction (change-score model: $F(1, 42) = 0.52$, $p = .47$; ANCOVA with baseline PHQ−9 as covariate: $F(1, 41) = 0.02$, $p = .90$). Because the two groups were selected at PHQ−9 extremes (0–2 vs. 5–19), this bidirectional pattern can be the result of regression to the mean and cannot be attributed specifically to negative movements. We therefore treat the follow-up PHQ−9 change as an exploratory observation rather than a movement-specific effect (see Discussion).

3.6. Post-hoc sensitivity analysis of group differences

To evaluate the magnitude and reliability of group differences, we calculated standardized effect sizes (Hedges' *g*) along with 95% confidence intervals for each primary comparison (Table 5). These were interpreted in relation to the design's minimum detectable effect sizes (MDEs; α =.05, power =.80) derived from the post-hoc sensitivity analysis. This approach allowed us to assess whether the observed effects exceeded the study's sensitivity threshold and to generalize their practical significance. For the negative emotional task β values, healthy subjects exhibited greater hemodynamic activation compared to symptomatic participants (β average of Healthy group = 11.5; β average of Symptomatic group = –18.8), corresponding to a large effect (Hedges' $g = 1.23$, 95% CI [0.39, 2.08]; Table 5). This observed effect exceeded the subgroup MDE ($d = 1.15$), suggesting adequate sensitivity for detecting group differences during negative emotional movements. In contrast, for the positive emotional movement task β values, the observed group difference was small (Hedges' $g = 0.26$, 95% CI [–0.57, 1.08]) and below the corresponding MDE ($d = 1.24$). This indicates that the positive-task comparison was underpowered, and subtle group differences in hemodynamic responses to positive emotional movements could not be reliably detected with the current sample size.

4. Discussion

As suggested by Charles Darwin, Antonio Damasio, William James, Carl Lange (Damasio, 1994; Damasio and Carvalho, 2013; Darwin, 1998; James, 1948) and supported by experimental evidence (Finzi and Rosenthal, 2016; Mennin et al., 2007; Duclos and Laird, 2001; McIntosh, 1996; Shafir, 2016; Shafir et al., 2013), our behavior shapes emotion. However, a mechanistic understanding of how bodily movements evoke emotional status has been elusive. By recording brain activity during emotional bodily movements using fNIRS, we found that negative emotional movements commonly activate the left anterior prefrontal cortex (Fig. 4). Interestingly, the same negative movements were associated with the opposite prefrontal response in subjects with elevated depressive symptoms: deactivation of this region. In an exploratory follow-up, depressive symptoms changed in opposite directions between the two groups (Fig. 5); however, because participants were selected at PHQ−9 extremes and both movement arms showed the same group-dependent pattern, this change could originate from the regression to the mean and thus cannot be interpreted as a movement-specific effect (see below). These results suggest that the left anterior prefrontal cortex shows a group-dependent, task-evoked response to negative emotional movements and may participate in brain–body interactions relevant to mood.

Previous studies have implicated left lateral prefrontal regions in depression and negative affective processing, frequently with a left-lateralized pattern. Using fMRI, Grimm et al. (2008) found that patients with major depressive disorder showed hypoactivity of the left, but not the right, dorsolateral prefrontal cortex specifically during

Table 4
Baseline PHQ−9, follow-up PHQ−9, and change scores for all four group × movement-valence cells. Δ, follow-up minus baseline PHQ−9; t and p are from within-cell two-tailed paired *t*-tests.

Cell(group × valence)	n	Baseline PHQ−9: Average (SD)	Follow-up PHQ−9: Average (SD)	Δ PHQ−9: Average (SD)	t (df)	p
Healthy–Negative	13	0.77 (0.83)	1.92 (1.66)	+ 1.15 (1.68)	2.47 (12)	.030
Healthy–Positive	13	0.69 (0.85)	1.00 (1.00)	+ 0.31 (0.85)	1.31 (12)	.213
Symptomatic–Negative	9	11.44 (3.05)	8.22 (3.46)	−3.22 (2.86)	−3.38 (8)	.010
Symptomatic–Positive	11	9.73 (2.49)	6.91 (3.11)	−2.82 (4.94)	−1.89 (10)	.088

Table 5
Summary of between-group comparisons for individual β values. Hedges' *g* is reported as an absolute effect size (healthy vs. symptomatic groups), together with its 95% confidence interval (CI) and the minimum detectable effect size (MDE) at 80% power. Effects with |*g*| exceeding the MDE indicate sufficient sensitivity; effects below the MDE were underpowered. The direction of each comparison is given in the main text.

	Number of subjects (Healthy / Symptomatic)	Healthy group: Average (SD)	Symptomatic group: Average (SD)	Hedges' g [95% CI]	MDE (80%)	Interpretation
β (Negative Task)	13 / 13	11.5 (20.9)	−18.8 (26.4)	1.23 [0.39, 2.08]	1.15	Exceeds MDE
β (Positive Task)	13 / 10	3.05 (101.0)	23.8 (22.7)	0.26 [−0.57, 1.08]	1.24	Below MDE

negative emotional judgment. Consistent with this, relatively reduced left frontal activation has long been described as a marker of depression and of diminished approach motivation (Henriques and Davidson, 1991), and the left lateral prefrontal cortex has been suggested to process depressive feelings while the right part serves a different role (Joos et al., 2012). This left-lateralized reduction of prefrontal engagement in depression parallels the deactivation of the left anterior prefrontal cortex that we observed in symptomatic subjects. Collectively, these studies indicate that left lateral prefrontal regions are engaged during negative affective processing, broadly consistent with the anterior prefrontal response we observed, rather than establishing that the left anterior prefrontal cortex mediates mood changes induced by negative emotional movements.

How can the imitation of the different negative emotional movements commonly activate the left anterior prefrontal cortex? The following mechanistic accounts are speculative and were not directly tested. One possibility is that the negative emotional movements share a common movement motif, which produces common proprioceptive feedback relayed to the anterior prefrontal cortex. This possibility is supported by evidence that proprioceptive feedback is associated with brain activity changes including the prefrontal cortex (Aman et al., 2015; Lial et al., 2017), and that all of the three negative emotional movements we used (hugging knees, sighing loudly, and drooping shoulders) commonly involve a shrinking posture and a slumped torso (Shafir, 2015).

As a further speculation, a candidate transduction pathway may relay proprioceptive feedback of negative emotional movements to the anterior prefrontal cortex. Proprioceptive signals from the limbs and torso ascend via the dorsal column-medial lemniscus pathway to the thalamus and primary somatosensory cortex, from which projections reach the insula, a region that processes proprioceptive signals and integrates them with emotional contexts (Tinaz et al., 2018; Kittleson et al., 2024). The insula projects densely to the orbitofrontal cortex (Chen et al., 2021); the anterior prefrontal cortex itself, however, connects predominantly with other prefrontal association areas rather than with sensory or interoceptive regions (Ramnani and Owen, 2004), so any influence of these proprioceptive and interoceptive signals on the anterior prefrontal cortex would be indirect (e.g., relayed via orbitofrontal or lateral prefrontal cortex) and remains speculative. Further research will be necessary to examine this possibility and to clarify how negative emotional movements are associated with common activation patterns in the prefrontal cortex.

Then, why did the imitation of the same negative emotional movements cause the opposite brain activity changes in symptomatic subjects? One possibility is that symptomatic subjects imitated the movements differently (e.g., with different kinematics), resulting in different proprioceptive feedback. However, it is hard to consider that the kinematics of the imitated movements, which were guided verbally and using videos, were different enough to cause the opposite proprioceptive feedback and opposite brain activity changes in the symptomatic subjects. An alternative possibility is that proprioceptive feedback from the similarly performed movements, or the feedback's impact on the left anterior prefrontal cortex, was the opposite in symptomatic subjects. Supporting this possibility, a study revealed that proprioceptive feedback can be changed during negative emotions (Ackerley et al., 2017), and a neuroimaging study reported altered prefrontal area (BA10) activation in patients with major depressive disorder (Katayama et al., 2019). Further investigations on the changes in individuals with elevated depressive symptoms in proprioceptive sensation, proprioceptive ascending circuitry, and the left anterior prefrontal cortex will decipher the in-depth mechanisms of the interesting phenomena we found.

An exploratory observation in this manuscript is that depressive symptoms changed in opposite directions in healthy and symptomatic subjects after the task, although, as noted above, this change could reflect regression to the mean (Fig. 5). One speculative interpretation, which we did not directly measure, invokes the concept of cognitive dissonance. Cognitive dissonance refers to a conflict between internal attitudes and external behaviors, which creates a feeling of mental discomfort as well as following efforts to match the internal state with external behaviors (Festinger, 1957; Harmon-Jones and Mills, 2019). In the present study, imitation of the negative emotional movements would allow symptomatic subjects to externalize their internal emotions. This might reduce cognitive dissonance during the movement, which can galvanize continued efforts to match external and internal status and thereby alleviate negative moods over the follow-up period (Greenberg et al., 2003; Greenberg and Vandekerckhove, 2008). Supporting this explanation, previous studies demonstrated that symptomatic subjects show reduced negative emotions after externalizing the emotions they felt internally (Greenberg and Vandekerckhove, 2008; Greenberg et al., 2003). In contrast, in the case of healthy subjects, imitating negative emotional movements might introduce a dissonance between their internal emotional state and external behavior. This induced dissonance could evoke discomfort, potentially resulting in a delayed increase in their PHQ−9 score. Further study might be necessary to address these possibilities and the role of the left anterior prefrontal activation in cognitive dissonance.

While the present findings provide novel insight into the distinct neural responses to negative emotional movements in healthy individuals and individuals with elevated depressive symptoms, these results should be interpreted with caution. First, the movement subgroups are small (approximately 13 participants per cell), and the key negative-task group difference (Hedges' g = 1.23) exceeds but lies close to its minimum detectable effect size (d = 1.15); this effect should therefore be regarded as provisional and requires replication in a larger, adequately powered sample. Second, because the groups were selected at the extremes of the PHQ−9 distribution (0–2 vs. 5–19), the follow-up PHQ−9 change is vulnerable to regression to the mean: the change tracked baseline symptom group in both movement arms, the valence × group interaction was non-significant, and no no-movement (passive re-test) control was included, so regression to the mean cannot be excluded as an explanation for the symptom change. Third, the follow-up interval was 1–2 weeks and was not held constant, and the PHQ−9 recall window partly overlaps the post-task period, so the delayed symptom change may also reflect uncontrolled life events, repeated-measurement reactivity, or expectancy effects. Fourth, the design is correlational with respect to the brain activity–symptom relationship, so we avoid causal and mediation language and treat the anterior

prefrontal cortex as a candidate correlate rather than a mediator. More clinically diverse cohorts, controlled follow-up intervals, and intervention-based or no-movement-control designs will be necessary to determine whether the opposing prefrontal responses represent a consistent pattern associated with elevated depressive symptoms and whether emotional movements causally influence mood.

A further consideration concerns the cultural generalizability of the emotional movements used in this study. The movements were selected based on publications conducted predominantly in Western research contexts (Coulson, 2004; Melzer et al., 2019; Shafir, 2015). Although the movements were primarily drawn from Western research contexts, several lines of evidence suggest that the negative emotional movements used in this study are likely to have cross-cultural relevance. The shrinking postures and slumped torso positions that characterize these movements have been shown to be reliably recognized as expressions of sadness and negative affect across diverse countries, including the United States, United Kingdom, Netherlands, China, Israel, Japan, and Nicaragua (Witkower et al., 2021). Consistent with this evidence, previous research has shown that similar postural cues are both recognized and produced across cultures. For example, Cordaro et al. (2018) identified a "slumped posture" as a core cross-cultural marker of sadness across multiple nations including Korea. Additionally, Tracy and Matsumoto (2008) suggested a possible biological basis for these movements by showing that a shame-related response, characterized by slumped shoulders and a narrowed chest, was observed after defeat across individuals from diverse cultures, including congenitally blind athletes who could not have learned these gestures through visual observation. Despite these findings provide support for the cross-cultural relevance of the negative emotional movements used in this study, subtle cultural modulations in the intensity or style of negative emotional movement expression might exist, limiting the generalizability of this study. Future studies directly comparing emotional movement-induced neural responses across cultural groups would strengthen the generalizability of the present findings.

To our knowledge, this is the first study to demonstrate brain activity changes associated with emotional bodily movements. This study identifies the left anterior prefrontal cortex as a candidate neural correlate associated with brain–body interaction relevant to depressive mood. Notably, the opposite prefrontal activation patterns observed between healthy and participants with elevated depressive symptoms suggest that emotional bodily movements may engage distinct regulatory mechanisms depending on affective state. This raises the possibility that movement-based interventions could be refined by tailoring emotional movement components to individuals' mental health status. Further studies on the brain-body interaction and its role in emotion will enable a comprehensive understanding of the origin of emotion and mood disorders, as well as engender behavior-based novel therapeutics for mood disorders.

Data and code availability

Prioritizing subject privacy, data access will be conditional upon approval by the corresponding author with a formal data sharing agreement. The software and code used in the study will be available upon request.

CRediT authorship contribution statement

Young-Gyun Park: Writing – review & editing, Writing – original draft, Supervision, Project administration, Conceptualization. **Nakyung Lee:** Methodology. **Hyuntae Jeong:** Methodology. **Hamin Park:** Investigation. **Ela li Maizel:** Writing – review & editing, Writing – original draft, Visualization, Investigation, Formal analysis, Data curation. **Somi Lee:** Writing – review & editing, Writing – original draft, Visualization, Methodology, Investigation, Formal analysis, Data curation. **Ratna Aditya Apsari:** Writing – original draft, Visualization, Software, Methodology, Investigation, Formal analysis, Data curation, Conceptualization.

Ethical statement

This study was conducted in accordance with the principles of the Declaration of Helsinki and received approval from the Institutional Review Board of KAIST. All participants signed written informed consent prior to the experiment, and the privacy rights of the subjects were observed.

Declaration of Generative AI and AI-assisted technologies in the writing process

During the preparation of this work, the authors used ChatGPT−4 in order to improve readability. After using this tool/service, the authors reviewed and edited the content as needed and take full responsibility for the content of the publication.

Funding

This work was supported by the National Research Foundation of Korea(NRF) grant funded by the Korea government(MSIT) (No. RS−2021-NR061634, RS−2024–00439379).

Declaration of Competing Interest

The authors declare that they have no known competing financial interests or personal relationships that could have appeared to influence the work reported in this paper.

Acknowledgements

We extend our gratitude to Hamin Park and Sooyeon Jeon of the Professor Young-Gyun Park's laboratory for the permission to use the photographs displayed in Fig. 1, Fig. 4, and Supplementary Figure 2.

Appendix A. Supporting information

Supplementary data associated with this article can be found in the online version at doi:10.1016/j.brainresbull.2026.112064.

References

Ackerley, R., Aimonetti, J.M., Ribot-Ciscar, E., 2017. Emotions alter muscle proprioceptive coding of movements in humans. Sci. Rep. 7, 8465. https://doi.org/10.1038/s41598-017-08721-4.

Al-Omairi, H.R., Fudickar, S., Hein, A., Rieger, J.W., 2023. Improved motion artifact correction in fNIRS data by combining wavelet and correlation-based signal improvement. Sensors 23, 3979. https://doi.org/10.3390/s23083979.

Aman, J.E., Elangovan, N., Yeh, I.-L., Konczak, J., 2015. The effectiveness of proprioceptive training for improving motor function: a systematic review. Front. Hum. Neurosci. 8, 1075. https://doi.org/10.3389/fnhum.2014.01075.

Baker, J.M., Bruno, J.L., Gundran, A., Hosseini, S.M.H., Reiss, A.L., 2018. fNIRS measurement of cortical activation and functional connectivity during a visuospatial working memory task. PLoS. ONE 13, e0201486. https://doi.org/10.1371/journal.pone.0201486.

Beard, C., Hsu, K.J., Rifkin, L.S., Busch, A.B., Björgvinsson, T., 2016. Validation of the PHQ-9 in a psychiatric sample. J. Affect. Disord. 193, 267–273. https://doi.org/10.1016/j.jad.2015.12.075.

Belleau, E.L., Treadway, M.T., Pizzagalli, D.A., 2019. The impact of stress and major depressive disorder on hippocampal and medial prefrontal cortex morphology. Biol. Psychiatry 85, 443–453. https://doi.org/10.1016/j.biopsych.2018.09.031.

Benedek, M., Kaernbach, C., 2010. A continuous measure of phasic electrodermal activity. J. Neurosci. Methods 190, 80–91. https://doi.org/10.1016/j.jneumeth.2010.04.028.

Caruelle, D., Gustafsson, A., Shams, P., Lervik-Olsen, L., 2019. The use of electrodermal activity (EDA) measurement to understand consumer emotions – A literature review and a call for action. J. Bus. Res. 104, 146–160. https://doi.org/10.1016/j.jbusres.2019.06.041.

Chen, W.G., Schloesser, D., Arensdorf, A.M., Simmons, J.M., Cui, C., Valentino, R., Gnadt, J.W., Nielsen, L., Hillaire-Clarke, C.S., Spruance, V., Horowitz, T.S.,

Vallejo, Y.F., Langevin, H.M., 2021. The emerging science of interoception: sensing, integrating, interpreting, and regulating signals within the self. Trends Neurosci. 44, 3–16. https://doi.org/10.1016/j.tins.2020.10.007.
Cohen, S., Kamarck, T., Mermelstein, R., 1983. A global measure of perceived stress. J. Heal. Soc. Behav. 24, 385–396.
Cordaro, D.T., Sun, R., Keltner, D., Kamble, S., Huddar, N., McNeil, G., 2018. Universals and cultural variations in 22 emotional expressions across five cultures. Emotion 18, 75–93. https://doi.org/10.1037/emo0000302.
Coulson, M., 2004. Attributing emotion to static body postures: recognition accuracy, confusions, and viewpoint dependence. J. Nonverbal Behav. 28, 117–139. https://doi.org/10.1023/b:jonb.0000023655.25550.be.
Damasio, A., Carvalho, G.B., 2013. The nature of feelings: evolutionary and neurobiological origins. Nat. Rev. Neurosci. 14, 143–152. https://doi.org/10.1038/nrn3403.
Damasio, A.R., 1994. Descartes' Error: Emotion, Reason, and the Human Brain. G.P. Putnam's Sons, New York.
Darwin, C., 1998. Expr. Emot. Man. Anim. https://doi.org/10.1093/oso/9780195112719.001.0001.
Delaveau, P., Jabourian, M., Lemogne, C., Guionnet, S., Bergouignan, L., Fossati, P., 2011. Brain effects of antidepressants in major depression: a meta-analysis of emotional processing studies. J. Affect. Disord. 130, 66–74. https://doi.org/10.1016/j.jad.2010.09.032.
Diener, C., Kuehner, C., Brusniak, W., Ubl, B., Wessa, M., Flor, H., 2012. A meta-analysis of neurofunctional imaging studies of emotion and cognition in major depression. NeuroImage 61, 677–685. https://doi.org/10.1016/j.neuroimage.2012.04.005.
Duclos, S.E., Laird, J.D., 2001. The deliberate control of emotional experience through control of expressions. Cogn. Emot. 15, 27–56. https://doi.org/10.1080/02699930126057.
Ferrari, M., Quaresima, V., 2012. A brief review on the history of human functional near-infrared spectroscopy (fNIRS) development and fields of application. NeuroImage 63, 921–935. https://doi.org/10.1016/j.neuroimage.2012.03.049.
Festinger, L., 1957. A Theory Cogn. Dissonance. https://doi.org/10.1515/9781503620766.
Finzi, E., Rosenthal, N.E., 2016. Emotional proprioception: treatment of depression with afferent facial feedback. J. Psy. Res. 93–96.
Fishburn, F.A., Ludlum, R.S., Vaidya, C.J., Medvedev, A.V., 2019. Temporal derivative distribution repair (TDDR): A motion correction method for fNIRS. NeuroImage 184, 171–179. https://doi.org/10.1016/j.neuroimage.2018.09.025.
Greenberg, L., Vandekerckhove, M., 2008. Regul. Emot. 240–268. https://doi.org/10.1002/9781444301786.ch10.
Greenberg, L.S., Elliott, R., Lietaer, G., 2003. Handb. Psychol. 301–325. https://doi.org/10.1002/0471264385.wei0812.
Grimm, S., Beck, J., Schuepbach, D., Hell, D., Boesiger, P., Bermpohl, F., Niehaus, L., Boeker, H., Northoff, G., 2008. Imbalance between left and right dorsolateral prefrontal cortex in major depression is linked to negative emotional judgment: an fMRI study in severe major depressive disorder. Biol. Psychiatry 63, 369–376. https://doi.org/10.1016/j.biopsych.2007.05.033.
Gu, Y., Miao, S., Han, J., Zeng, K., Ouyang, G., Yang, J., Li, X., 2017. Complexity analysis of fNIRS signals in ADHD children during working memory task. Sci. Rep. 7, 829. https://doi.org/10.1038/s41598-017-00965-4.
Harmon-Jones, E., Mills, J., 2019. An introduction to cognitive dissonance theory and an overview of current perspectives on the theory. In: Harmon-Jones, E. (Ed.), Cognitive dissonance: Reexamining a pivotal theory in psychology, 2nd ed, pp. 3–24. https://doi.org/10.1037/0000135-001.
Hennenlotter, A., Dresel, C., Castrop, F., Ceballos-Baumann, A.O., Baumann, A.O.C., Wohlschläger, A.M., Haslinger, B., 2009. The link between facial feedback and neural activity within central circuitries of emotion—new insights from botulinum toxin–induced denervation of frown muscles. Cereb. Cortex 19, 537–542. https://doi.org/10.1093/cercor/bhn104.
Henriques, J.B., Davidson, R.J., 1991. Left frontal hypoactivation in depression. J. Abnorm. Psychol. 100, 535–545. https://doi.org/10.1037/0021-843X.100.4.535.
Huang, R., Hong, K.-S., Yang, D., Huang, G., 2022. Motion artifacts removal and evaluation techniques for functional near-infrared spectroscopy signals: a review. Front. Neurosci. 16, 878750. https://doi.org/10.3389/fnins.2022.878750.
James, W., 1948. Read. Hist. Psychol. 290–303. https://doi.org/10.1037/11304-033.
Joos, K., Vanneste, S., Ridder, D.D., 2012. Disentangling depression and distress networks in the tinnitus brain. PLoS. ONE 7, e40544. https://doi.org/10.1371/journal.pone.0040544.
Katayama, N., Nakagawa, A., Umeda, S., Terasawa, Y., Kurata, C., Tabuchi, H., Kikuchi, T., Mimura, M., 2019. Frontopolar cortex activation associated with pessimistic future-thinking in adults with major depressive disorder. NeuroImage Clin. 23, 101877. https://doi.org/10.1016/j.nicl.2019.101877.
Khalsa, S.S., Adolphs, R., Cameron, O.G., Critchley, H.D., Davenport, P.W., Feinstein, J. S., Feusner, J.D., Garfinkel, S.N., Lane, R.D., Mehling, W.E., Meuret, A.E., Nemeroff, C.B., Oppenheimer, S., Petzschner, F.H., Pollatos, O., Rhudy, J.L., Schramm, L.P., Simmons, W.K., Stein, M.B., Stephan, K.E., Van den Bergh, O., Van Diest, I., von Leupoldt, A., Paulus, M.P., 2018. Interoception and mental health: a roadmap. Biol. Psychiatry Cogn. Neurosci. Neuroimaging 3, 501–513. https://doi.org/10.1016/j.bpsc.2017.12.004.
Kittleson, A.R., Woodward, N.D., Heckers, S., Sheffield, J.M., 2024. The insula: leveraging cellular and systems-level research to better understand its roles in health and schizophrenia. Neurosci. Biobehav. Rev. 160, 105643. https://doi.org/10.1016/j.neubiorev.2024.105643.
Kroenke, K., Spitzer, R.L., Williams, J.B., 2001. The PHQ-9: validity of a brief depression severity measure. J. Gen. Intern. Med. 16, 606–613. https://doi.org/10.1046/j.1525-1497.2001.016009606.x.
Laird, J.D., Lacasse, K., 2014. Bodily Influences on Emotional Feelings: Accumulating Evidence and Extensions of William James's Theory of Emotion. Emot. Rev. 6, 27–34. https://doi.org/10.1177/1754073913494899.
Lee, G., Jin, S.H., Yang, S.T., An, J., Abibulaev, B., 2018. Cross-Correlation Between HbO and HbR as an effective feature of motion artifact in fNIRS Signal. 2018 6th Int. Conf. Brain-Comput. Interface (BCI) 1–3. https://doi.org/10.1109/iww-bci.2018.8311513.
Lee, T.-W., Josephs, O., Dolan, R.J., Critchley, H.D., 2006. Imitating expressions: emotion-specific neural substrates in facial mimicry. Soc. Cogn. Affect. Neurosci. 1, 122–135. https://doi.org/10.1093/scan/nsl012.
Lial, L., Moreira, R., Correia, L., Andrade, A., Pereira, A.C., Lira, R., Figueiredo, R., Silva-Júnior, F., Orsini, M., Ribeiro, P., Velasques, B., Cagy, M., Teixeira, S., Bastos, V.H., 2017. Proprioceptive neuromuscular facilitation increases alpha absolute power in the dorsolateral prefrontal cortex and superior parietal cortex. Somatosens. Mot. Res. 34, 204–212. https://doi.org/10.1080/08990220.2017.1392298.
Magyar-Moe, J.L., 2009. Therapist's Guide to Positive Psychological Interventions, pp. 43–72. https://doi.org/10.1016/b978-0-12-374517-0.00003-6.
McIntosh, D.N., 1996. Facial feedback hypotheses: evidence, implications, and directions. Motiv. Emot. 20, 121–147. https://doi.org/10.1007/bf02253868.
Melzer, A., Shafir, T., Tsachor, R.P., 2019. How do we recognize emotion from movement? specific motor components contribute to the recognition of each emotion. Front. Psychol. 10, 1389. https://doi.org/10.3389/fpsyg.2019.01389.
Mennin, D.S., Holaway, R.M., Fresco, D.M., Moore, M.T., Heimberg, R.G., 2007. Delineating components of emotion and its dysregulation in anxiety and mood psychopathology. Behav. Ther. 38, 284–302. https://doi.org/10.1016/j.beth.2006.09.001.
Merz, E.L., Malcarne, V.L., Roesch, S.C., Ko, C.M., Emerson, M., Roma, V.G., Sadler, G.R., 2013. Psychometric properties of Positive and Negative Affect Schedule (PANAS) original and short forms in an African American community sample. J. Affect. Disord. 151, 942–949. https://doi.org/10.1016/j.jad.2013.08.011.
Meyer, T.J., Miller, M.L., Metzger, R.L., Borkovec, T.D., 1990. Development and validation of the penn state worry questionnaire. Behav. Res. Ther. 28, 487–495. https://doi.org/10.1016/0005-7967(90)90135-6.
Obrig, H., Wenzel, R., Kohl, M., Horst, S., Wobst, P., Steinbrink, J., Thomas, F., Villringer, A., 2000. Near-infrared spectroscopy: does it function in functional activation studies of the adult brain? Int. J. Psychophysiol. 35, 125–142. https://doi.org/10.1016/S0167-8760(99)00048-3.
Odero, S.A., Mwangi, P., Odhiambo, R., Nzioka, B.M., Shumba, C., Ndirangu-Mugo, E., Abubakar, A., 2023. Psychometric evaluation of PHQ–9 and GAD–7 among community health volunteers and nurses/midwives in Kenya following a nation-wide telephonic survey. Front. Psychiatry 14, 1123839. https://doi.org/10.3389/fpsyt.2023.1123839.
Oniz, A., Inanc, G., Taslica, S., Guducu, C., Ozgoren, M., 2019. Sleep is a refreshing process: an fNIRS Study. Front. Hum. Neurosci. 13, 160. https://doi.org/10.3389/fnhum.2019.00160.
Pinti, P., Aichelburg, C., Lind, F., Power, S., Swingler, E., Merla, A., Hamilton, A., Gilbert, S., Burgess, P., Tachtsidis, I., 2015. Using fiberless, wearable fNIRS to monitor brain activity in real-world cognitive tasks. J. Vis. Exp. (106), e53336. https://doi.org/10.3791/53336.
Pinti, P., Aichelburg, C., Gilbert, S., Hamilton, A., Hirsch, J., Burgess, P., Tachtsidis, I., 2018. A Review on the Use of Wearable Functional Near-Infrared Spectroscopy in Naturalistic Environments. Jpn Psychol. Res. 60, 347–373. https://doi.org/10.1111/jpr.12206.
Pinti, P., Tachtsidis, I., Hamilton, A., Hirsch, J., Aichelburg, C., Gilbert, S., Burgess, P.W., 2020. The present and future use of functional near-infrared spectroscopy (fNIRS) for cognitive neuroscience. Ann. N. Y. Acad. Sci. 1464, 5–29. https://doi.org/10.1111/nyas.13948.
Ramnani, N., Owen, A.M., 2004. Anterior prefrontal cortex: insights into function from anatomy and neuroimaging. Nat. Rev. Neurosci. 5, 184–194. https://doi.org/10.1038/nrn1343.
Santosa, H., Zhai, X., Fishburn, F., Huppert, T., 2018. The NIRS Brain AnalyzIR Toolbox. Algorithms 11, 73. https://doi.org/10.3390/a11050073.
Santosa, H., Zhai, X., Fishburn, F., Sparto, P.J., Huppert, T.J., 2020. Quantitative comparison of correction techniques for removing systemic physiological signal in functional near-infrared spectroscopy studies. Neurophotonics 7, 035009. https://doi.org/10.1117/1.nph.7.3.035009.
Scholkmann, F., Kleiser, S., Metz, A.J., Zimmermann, R., Pavia, J.M., Wolf, U., Wolf, M., 2014. A review on continuous wave functional near-infrared spectroscopy and imaging instrumentation and methodology. Neuroimage 85, 6–27. https://doi.org/10.1016/j.neuroimage.2013.05.004.
Shafir, T., 2015. Movement-based Strategies for Emotion Regulation. In: Bryant, M.L. (Ed.), Handbook on Emotion Regulation, Handbook on Emotion Regulation, pp. 232–249.
Shafir, T., 2016. Using Movement to Regulate Emotion: Neurophysiological Findings and Their Application in Psychotherapy. Front. Psychol. 7, 1451. https://doi.org/10.3389/fpsyg.2016.01451.
Shafir, T., Taylor, S.F., Atkinson, A.P., Langenecker, S.A., Zubieta, J.-K., 2013. Emotion regulation through execution, observation, and imagery of emotional movements. Brain Cogn. 82, 219–227. https://doi.org/10.1016/j.bandc.2013.03.001.
Shafir, T., Tsachor, R.P., Welch, K.B., 2016. Emotion regulation through movement: unique sets of movement characteristics are associated with and enhance basic emotions. Front. Psychol. 6, 2030. https://doi.org/10.3389/fpsyg.2015.02030.
Sheehan, D.V., Lecrubier, Y., Sheehan, K.H., Amorim, P., Janavs, J., Weiller, E., Hergueta, T., Baker, R., Dunbar, G.C., 1998. The Mini-International Neuropsychiatric Interview (M.I.N.I.): the development and validation of a

structured diagnostic psychiatric interview for DSM-IV and ICD-10. J. Clin. Psychiatry 59 (20), 34–57, 22-33;quiz.
Spitzer, R.L., Kroenke, K., Williams, J.B.W., Löwe, B., 2006. A brief measure for assessing generalized anxiety disorder: the GAD-7. Arch. Intern. Med. 166, 1092–1097. https://doi.org/10.1001/archinte.166.10.1092.
Tak, S., Ye, J.C., 2014. Statistical analysis of fNIRS data: a comprehensive review. NeuroImage 85, 72–91. https://doi.org/10.1016/j.neuroimage.2013.06.016.
Tinaz, S., Para, K., Vives-Rodriguez, A., Martinez-Kaigi, V., Nalamada, K., Sezgin, M., Scheinost, D., Hampson, M., Louis, E.D., Constable, R.T., 2018. Insula as the interface between body awareness and movement: a neurofeedback-guided kinesthetic motor imagery study in Parkinson's disease. Front. Hum. Neurosci. 12, 496. https://doi.org/10.3389/fnhum.2018.00496.
Tracy, J.L., Matsumoto, D., 2008. The spontaneous expression of pride and shame: evidence for biologically innate nonverbal displays. Proc. Natl. Acad. Sci. 105, 11655–11660. https://doi.org/10.1073/pnas.0802686105.
Veenstra, L., Schneider, I.K., Koole, S.L., 2016. Embodied mood regulation: the impact of body posture on mood recovery, negative thoughts, and mood-congruent recall. Cogn. Emot. 31, 1–16. https://doi.org/10.1080/02699931.2016.1225003.
Watson, D., Clark, L.A., Tellegen, A., 1988. Development and validation of brief measures of positive and negative affect: the PANAS Scales. J. Pers. Soc. Psychol. 54, 1063–1070. https://doi.org/10.1037/0022-3514.54.6.1063.
Witkower, Z., Hill, A.K., Koster, J., Tracy, J.L., 2021. Beyond face value: evidence for the universality of bodily expressions of emotion. Affect. Sci. 2, 221–229. https://doi.org/10.1007/s42761-021-00052-y.
Wyser, D., Mattille, M., Wolf, M., Lambercy, O., Scholkmann, F., Gassert, R., 2020. Short-channel regression in functional near-infrared spectroscopy is more effective when considering heterogeneous scalp hemodynamics. Neurophotonics 7, 035011. https://doi.org/10.1117/1.nph.7.3.035011.
Wyser, D.G., Kanzler, C.M., Salzmann, L., Lambercy, O., Wolf, M., Scholkmann, F., Gassert, R., 2022. Characterizing reproducibility of cerebral hemodynamic responses when applying short-channel regression in functional near-infrared spectroscopy. –015004 Neurophotonics 9, 015004. https://doi.org/10.1117/1.nph.9.1.015004.